Photoluminescence from MoS_2 nanostructures prepared via top-down approach

Shubham Bhagat, Shivani Sharma, Jasvir Singh, and Sandeep Sharma[1]
[1]Department of Physics, Guru Nanak Dev University, Amritsar, Punjab- 143005
[1]Email: sandeepscl@gmail.com

Abstract— Highly crystalline nanostructures of MoS_2 have been synthesized using combined process of high energy ball-milling and probe sonication. The nanostructures so formed display excitonic absorptions together with band edge absorption at ≈ 2.82 eV, sufficiently larger than band gap for a monolayer MoS_2. These nanostructures exhibit photoluminescence emission that varies with the excitation wavelength, a signature of polydisperse nature of MoS_2 nanostructures. Further, raman spectra revealed the presence of various first-order and second-order raman modes.

Index Terms— Band gap, Excitons, nanostructures, photoluminescence, quantum dots, raman active modes, XRD

1 Introduction

FOR many years the existence of free standing two dimensional (2D) systems were thought of as a hypothetical concept, the reason being the thermal fluctuations. But the realization of isolated graphene sheets by exfoliation of weakly bonded graphite exposed new potentials of 2D systems. Graphene a 2-D material, possesses a very large mobility (≈ 10^5 $cm^2V^{-1}s^{-1}$), but the absence of band gap in pristine material make it unsuitable for many device related applications. Although bandgap in graphene can be introduced by various methods, including application of external electric field, nanostructuring and chemical functionalization etc, but at the cost of reduced mobility [1], [2], [3]. This limitation of graphene has stimulated research interests in other inorganic 2D materials such as transition-metal di-chalcogenides (TMDCs) [4], [5] of the type MX_2. Here, M is the transition metal either from group IVB, VB, or VIB and X is chalcogens such as S, Se and so on from group VIA. The class of TMDCs compounds spans a wide range of materials from metals, semi-metals, insulators and superconductors to semiconductors. The reason for this wide range of electrical properties can be attributed to the number of d-electrons of transition metal and different polytypes of TMDCs.

Of the different materials from TMDC family, semiconducting MoS_2 and WS_2 are the materials that has been studied extensively. The 2D form of TMDC's has attracted extensive scientific attention due to their diverse electronic [6], catalytic [7], [8], [9] and optical properties.

The bulk MoS_2 belonging to the space group P63/mmc, is an indirect band gap semiconductor with band gap of 1.29 eV whereas on reducing it to monolayer it turns out to be a direct band gap semiconductor with increased band gap of 1.9 eV [9]. The direct band gap of the TMDCs in monolayer form lies in the visible region of the spectrum. For this reason, TMDCs are considered as best candidates for photodetectors and other light sensitive applications.

Owing to its indirect band gap in bulk MoS_2, the photoluminescence is quite feeble to be detected. However, in monolayer form the photoluminescence emerges in these material, a direct consequence of direct band gap in monolayer. This is indeed supported by various recent studies showing emergence of photoluminescence in ultrathin layers of MoS_2. These changes are attributed to the modified electronic structures in monolayered form. Therefore, in monolayerd form these materials offers a unique platform to exploit their electric as well as optical properties. It will be even more interesting, if the dimensions of these materials can be further reduced to nano regime. The interests in these nanostructured materials arises from the fact that they possess fascinating fundamental physical properties that offer applications not only in the electronic industry but also in some biological applications. For e.g. various applications of TMDCs nanostructures in the field of biological sensors, carriers in nanomedicines [10], [11], [12] and band selective absorption [13] have been introduced. Various methods can be used for the synthesis of these nanostructures. We have used the top-down approach, where we begin with a bulk crystalline material and use highly energetic ball-milling and probe sonication to reduce the thickness of the starting material. In ball milling, the powdered sample is subjected to high energy collision by the zirconium balls. Balls apply shear and compression forces on the sample, and may damage the structure of initial material.

Here, in present work, we report the synthesis of highly crystalline MoS_2 nanosheets/quantum-dots hybrids using combined process of highly energetic ball-milling and probe-sonication process. We will provide a detailed discussion on structural and optical properties of MoS_2 nanostructures. First, in experimental section, we will describe the synthesis method and sample preparation. This is followed by discussion on structural and optical properties of the MoS_2 nanostructures

2 Experimental

Bulk crystalline powder of MoS_2 was purchased from Sigma Aldrich. Further 2.5 gm of Sigma MoS_2 was mixed with isopropyl alcohol and the mixture was grinded using high energy ball milling for 30 hours at 250 rpm. Thereafter the grinded sample was dried in air. A part of this ball milled sample was used for X-rays diffraction and Raman spectroscopic measurements. We took 1 gm MoS_2 from the ball-milled powder and mixed it with 60 ml of Dimethylformamide (DMF) to further process it with high energy (750 Watt, 20 kHz) probe sonicator (PCI-Analytics, India) for two and half hours. This resulted in a yellow coloured suspension in DMF along with thin sheets of MoS_2 floating on the surface of DMF. This suspension was allowed to settle at room temperature for three days. The floating sheets of MoS_2 were transferred on Si substrate via dip coating. From the yellow coloured suspension, sample S1 was taken out and

remained suspension was further processed for another one hour to obtain sample S2. These two samples were used for structural and optical characterization of the nanostructures.

The structural analysis of the obtained samples was carried out using X-ray diffraction (XRD) and high resolution transmission electron microscope (HRTEM). XRD was performed using D8 Focus Diffractometer using Cu K_α radiation (λ= 0.154 nm). Transmission electron microscopic imaging was performed using JEOL (JEM-2100). Renishaw Invia Reflex micro Raman spectrometer was used to study the various vibrational modes in synthesized samples using excitation wavelength of 514 nm. Optical characterization of the samples was carried out using Shimadzu UV-Vis-2450 spectrophotometer and photoluminsence emission pattern was recorded using Perkin Elmer LS55 fluorescence Spectrometer.

3 Results and Discussions

3.1 X-Ray Diffraction

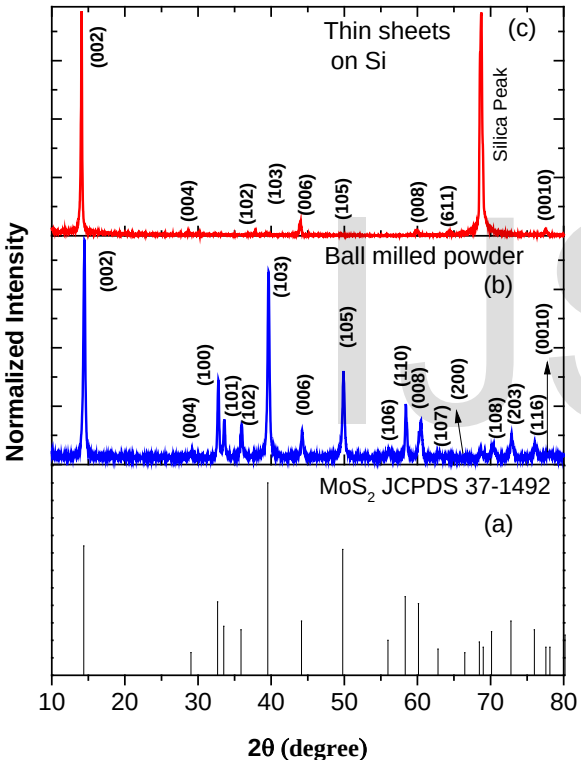

Fig. 1. (color online) XRD pattern of MoS_2 (a) Standard data JCPDS-37-1492, (b) Ball milled powder, (c) Thin flakes transferred on Si-substrate.

Fig.1 compares the XRD patterns of bulk crystalline sample, ball-milled powder and thin nano sheets transferred on silicon substrate. The XRD peaks in ball milled sample can be indexed with (JCPDS-37-1492) highly crystalline hexagonal structure belonging to P63/mmc space group. Intense (002) peak indicates the dominant contribution from (002) planes in the crystalline sample. Compared to peak intensity from (002) planes, other peaks have relatively lesser intensity.

3.2 Transmission Electron Microscopy

Morphological and crystal structure analysis was carried out using High Resolution Transmission Electron Microscopy (HRTEM). Fig.2 displays the TEM images from MoS_2 samples taken at different magnifications. Fig.2 (a) illustrates the low resolution image of the layered nanosheets, whereas Fig.2 (b) shows the image of agglomerated quantum dots. In Fig.2 (c) a high resolution image of a quantum dot is shown. The quantum dots so obtained are circular in shape and size is of the order or 12 nm. The lattice fringe spacing is of the order of 2.76 Å.

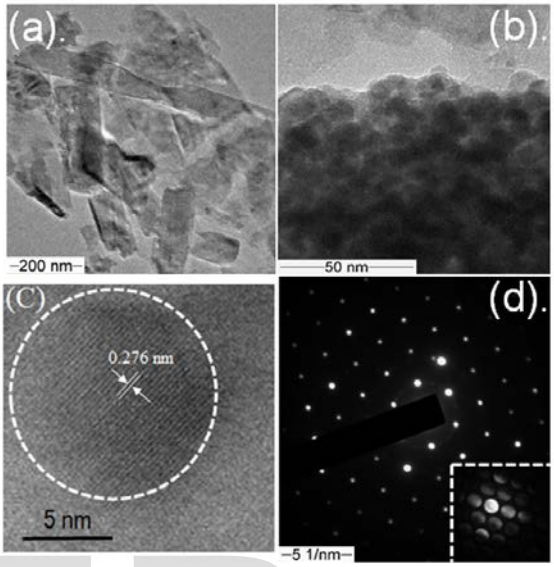

Fig. 2. (color online) TEM images of MoS_2 (a) Low resolution image of nanoflakes, (b) agglomerated quantum dots, (c) high resolution image of individual quantum dots, and (d) Selected area electron diffraction pattern.

3.3 Raman spectroscopy

Fig.3 (a) and (b) shows the raman spectra of bulk and grinded powder of MoS_2. The spectra were acquired at room temperature with excitation wavelength λ_{exc} =514nm. As we see, both samples display, two first-order dominant modes E^1_{2g} and A_{1g} at Γ point of Brillouin zone. As we see, the raman spectra for ball milled sample contains more modes, revealing many second-order peaks compared to bulk sample. Symmetry assignments for various raman modes are given in Fig.3. Three first order raman active modes E_{1g}, E^1_{2g} and A_{1g} at 283.12, 378.36 and 404.80 cm^{-1}, respectively are observed in grinded powder of MoS_2. We didn't observe the raman active mode E_{2g} at 32 cm^{-1}, as it is forbidden in back scattered geometry [14].

In addition to first order modes, the second order modes were also observed which arise because of the disorder. The disorder at the edges is likely to be introduced in the sample from high energy ball milling followed by probe sonication. These second order modes arise from the combination of first order modes and zone edge mode activated by disorder. The latter has been identified as longitudinal acoustic phonon mode at M point of the Brillouin zone (LA(M)), arising from the collective movement of the atoms within the lattice. The mode at 447.21 and 589.51 cm^{-1} are identified as 2LA(M) and E^1_{2g} + LA(M) [16] respectively. Other higher frequency modes at 820.46, and 993.56 cm^{-1} are identified as arising from the vibration of oxidized Mo. The higher laser power may likely cause the oxidation of MoS_2 into MoO_3 and give rise to the observed mode [17]. The raman peaks at 336.26, 283.12, 148.25 and 124.31cm^{-1} are attributed to E_{2u} [18], E_{1g}, E^1_{2g} - LA (M) and E^1_{2g} - A_{1g} combination modes [19], respectively.

As we see in Fig. 2(b), the E^1_{2g} and A_{1g} modes in ball-milled sample are red shifted w.r.t to the bulk sample. The A_{1g} mode has shown a red shift of 4.99 cm^{-1} as compared to bulk. Whereas E^1_{2g} mode is red shifted by 5.14 cm^{-1} w.r.t bulk sample. The in-plane mode E^1_{2g} and out-of plane mode A_{1g} are expected to stiffen with the increasing number of layers, due to the increased magnitude of Van-der-Waals force between the layers [20], [21]. However, in our case, both the raman active modes E^1_{2g} and A_{1g} stiffened on moving from few layer to bulk form of MoS_2, thus implying the dominance of Van der Waals forces in bulk layered sample.It should be noted that anomalous shift in these modes has been pointed out by various other research

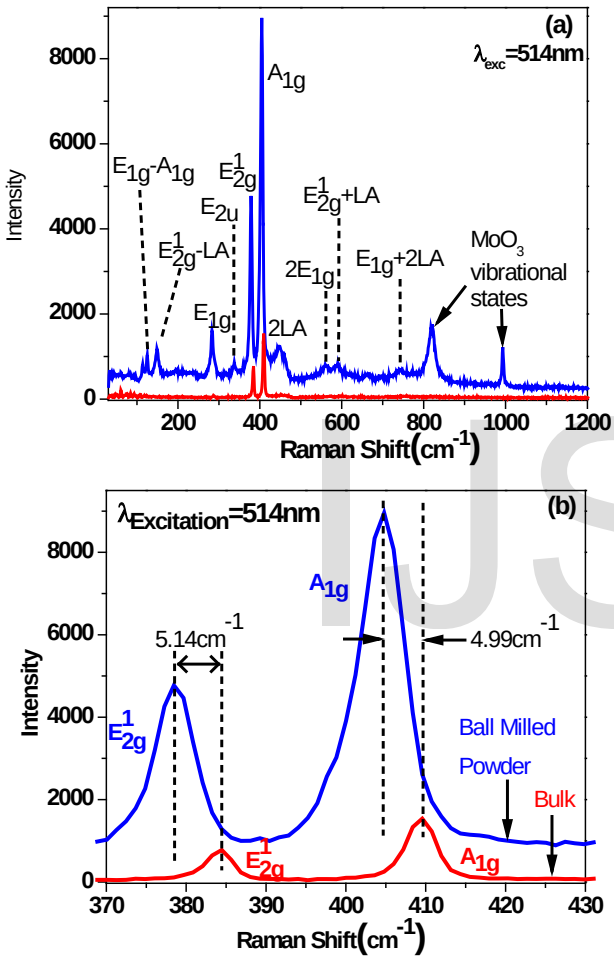

Fig. 3. (color online) Raman spectra of MoS_2 (a) bulk and ball milled powder, (b) Shift in raman peaks for bulk and grinded powder.

groups. For e.g.Lee et. al [15] has shown that E^1_{2g} mode softens (red shifts), while A_{1g} mode stiffens with increased sample thickness. Cheng et. al [21] has explained the observed shift by considering the reduced interlayer coupling for monolayer sample.

3.4 UV- Vis Spectroscopy

Fig.4 shows the UV-Vis spectra of MoS_2 nanostructures, obtained at different sonication time.

The samples S1 was collected after two and half hours whereas S2 was collected after three and half hours of probe sonication. The absorption spectra of sample S1 depicts two absorption peaks at 683.2 nm (1.82eV) and 624.6 nm (1.99eV). These absorption peaks are identified as excitonic absorption 'A' and 'B', respectively. They arise from spin-orbit-coupling induced (SOC) splitting of the valence band at the K point of the Brillouin zone [22]. The separation between these two peaks is ≈ 170 meV, in agreement with the theoretical calculations [23]. Another absorption hump can be seen around ≈ 471 nm (2.64 eV) and might be due to higher excited state of the excitons [24]. Similar measurements on sample S2 yielded two excitonic absorptions at 681 nm (1.82 eV) and 617.6 nm (2.01 eV). The band edge absorption for this sample is obtained at ≈ 440 nm (2.82 eV), a bit larger than the value obtained for sample S1. It is interesting to note that band edge absorption (2.76 eV and 2.82 eV for S1 and S2) is much higher than the band gap (≈ 1.89 eV) for a monolayer. This increase in band gap is due to the fact that high energy ball milling together with probe sonication has significantly decreased the crystallite size down to the nanometer regime where quantum confinement effects plays a major role in determining the optical absorption within the material. In sample S2, another absorption appear at ≈ 983 nm. This absorption occurs due to indirect transitions from point between Γ and K point of the Brillouin zone of the

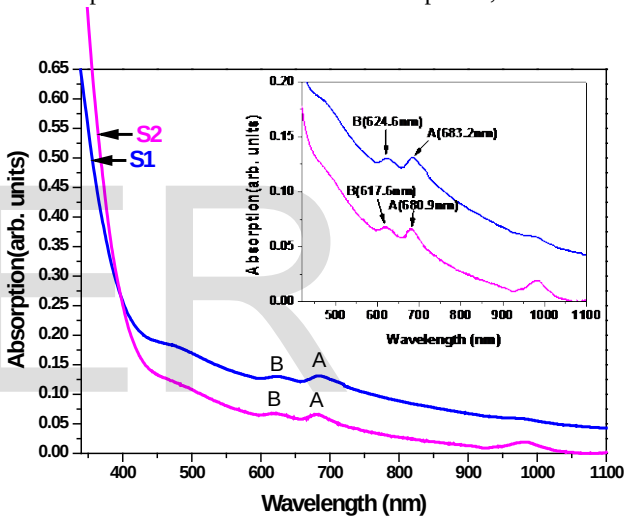

Fig. 4. (color online) UV-Vis spectra of MoS_2 nanostructures.

valence band to the K point of the conduction band minima [25]. Therefore, we see that with increase in sonication time the absorption edge has shifted to lower wavelength. And this shift is attributed to the quantum confinement effects within the nanostructures of MoS_2.

3.5 Photoluminescence Spectroscopy

Fig. 5 (a) and (b) depicts the photoluminescence emission spectra of MoS_2 nanostructures at different excitation wavelengths. As we see the emission pattern shifts with the excitation wavelength. At lower excitation wavelength (λ_{exc}= 300nm), the emission covers a wider range and maxima occurs around 400 nm. With increase in the excitation wavelength the emission pattern shifts to higher wavelengths and new maxima occurs at ≈ 430 nm for λ_{exc}=350 nm. As we see, the intensity of emission also reduces with increase in excitation wavelength. Similar features are observed in Fig. 5(b). Therefore, we observed that emission spectra of the prepared MoS_2 nanostructures

shifts to higher wavelength as the excitation wavelength is increased. The MoS_2 nanostructures have a variable size. The smaller nanostructures (quantum dots) have larger band gap whereas large size nanostructures or nanosheets will have a bit smaller band gap. This polydispersity of the nanostructures make the emission spectra to be excitation dependent. At lower excitation wavelength the structures with larger bandgap are excited whereas at larger wavelength the larger size nanostructures are excited. This size selective excitation give rise to the observed emission pattern in the nanostructures.

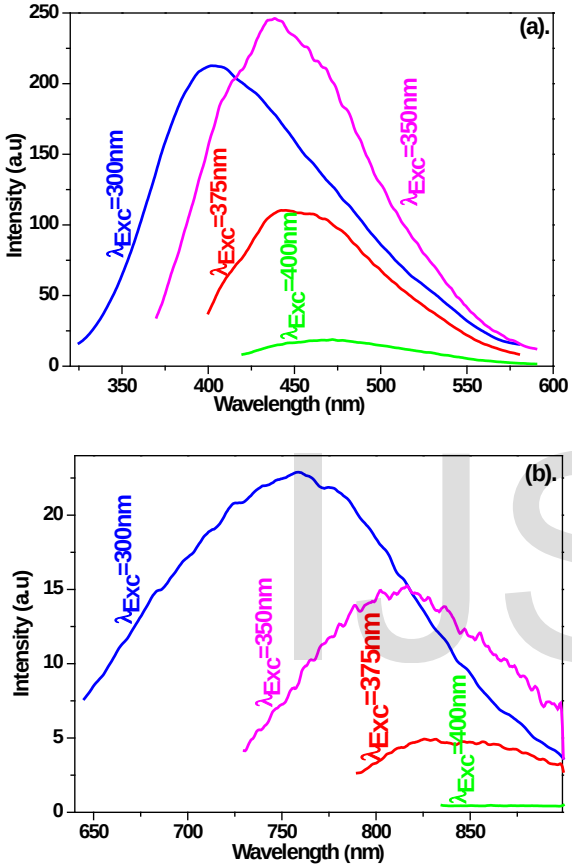

Fig. 5. (color online) (a) and (b) Photoluminescence spectra from MoS_2 nanostructures at different excitaion wavelength.

4 Conclusion

We have shown the synthesis of MoS_2 nanostructures by combining the process of high energy ball milling and probe sonication. The nano structures so obtained are highly crystalline in nature and possess six-fold symmetry. These nanostructures display excitonic features their absorption spectrum together with the band edge absorption at ≈ 2.89 eV, sufficiently larger than the band gap for a monolayer MoS_2. The increased band gap is attributed to the quantum confinement effects within the nanostructures. Further the photoluminescence emission spectra confirms the polydisperse nature of the nanostructures.

Acknowledgment

One of the authors, Shubham Bhagat, acknowledges Guru Nanak Dev University for providing the research grant under UPE Scheme.

References

[1] Q. H. Wang, K. Kalantar Zadeh, A. Kis, J. N. Coleman, and M. S. Strano, " Electronics and optoelectronics of two-dimensional transition metal dichalcogenides", Nat Nano, 7, 699, 2012.

[2] M. Y. Han, B. Ozyilmaz, Y. Zhang, and P. Kim, "Energy Band-Gap Engineering of Graphene Nanoribbons", Phys. Rev. Lett., 98, 206805, 2007.

[3] M.W. Lin, C. Ling, Y. Zhang, H. J. Yoon, M. M.C. Cheng, L. A. Agapito, N. Kioussis, N. Widjaja, and Z. Zhou, "Room-temperature high on/off ratio in suspended graphene nanoribbon field-effect transistors", Nanotechnology, 22, 265201, 2011.

[4] K. S. Novoselov, V. I. Fal[prime]ko, L. Colombo, P. R. Gellert, M. G. Schwab, and K. Kim, "A roadmap for graphene" , Nature 490, 192 (2012).

[5] F. Schwierz, "Graphene transistors", Nat Nano 5, 487, 2010.

[6] T. Li and G. Galli, "Electronic Properties of MoS_2 Nanoparticles", J. Phys. Chem, 111 (44), 16192-16196, 2007.

[7] P. Raybaud, J. Hafner, G. Kresse, S. Kasztelan, and H. Toulhoat, "Ab Initio Study of the H_2-H_2S/MoS_2 Gas-Solid Interface: The Nature of the Catalytically Active Sites", Journal of Catalysis, 189, 129, 2000.

[8] M. Sun, A. E. Nelson, and J. Adjaye, "Ab initio DFT study of hydrogen dissociation on MoS_2, NiMoS, and CoMoS: mechanism, kinetics, and vibrational frequencies", Journal of Catalysis, 233, 411, 2005.

[9] E. S. Kadantsev and P. Hawrylak, "Electronic structure of a single MoS_2 monolayer", Solid State Communications, 152, 909, 2012.

[10] Y. Yong, X. Cheng, T. Bao, M. Zu, L. Yan, W. Yin, C. Ge, D. Wang, Z. Gu, and Y. Zhao, "Tungsten Sulfide Quantum Dots as Multifunctional Nanotheranostics for In Vivo Dual-Modal Image- Guided Photothermal/ Radiotherapy Synergistic Therapy", ACS Nano ,9, 12451, 2015.

[11] Z. X. Gan, L. Z. Liu, H. Y. Wu, Y. L. Hao, Y. Shan, X. L. Wu, and P. K. Chu, "Quantum confinement effects across two-dimensional planes in MoS_2 quantum dots" ,Applied Physics Letters, 106, 233113, 2015.

[12] V. Stengl and J. Henych, "Strongly luminescent monolayered MoS_2 prepared by effective ultrasound exfoliation", Nanoscale 5, 3387, 2013.

[13] D. B. Velusamy, R. H. Kim, S. Cha, J. Huh, R. Khazaeinezhad, S. H. Kassani, G. Song, S. M. Cho, S. H. Cho, I. Hwang, J. Lee, K. Oh, H. Choi, and C. Park, "Flexible transition metal dichalcogenide nanosheets for band-selective photodetection" ,Nature Communications, 6, 8063, 2015.

[14] H. Li, Q. Zhang, C. C. R. Yap, B. K. Tay, T. H. T. Edwin, A. Olivier, and D. Baillargeat, "From Bulk to Monolayer MoS_2: Evolution of Raman Scattering" Advanced Functional Materials 22, 1385 (2012)

[15] C. Lee, H. Yan, L. E. Brus, T. F. Heinz, J. Hone, and S. Ryu, "Anomalous Lattice Vibrations of Single- and Few-Layer MoS_2", ACS Nano 4, 2695 (2010)

[16] A. Bera and A. K. Sood, "Insights into vibrational and electronic properties of MoS_2 using raman, photoluminescence, and transport studies," in MoS_2: Materials, Physics and Devices, edited by Z. M. Wang, Springer International Publishing,155-215, 2014.

[17] B. C. Windom, W. G. Sawyer, and D. W. Hahn, Tribology Letters, "A Raman Spectroscopic Study of MoS_2 and MoO_3: Applications to Tribological Systems", 42, 301, 2011.

[18] M. Placidi, M. Dimitrievska, Victor Izquierdo-Roca, Xavier Fontané, Andres Castellanos-Gomez, Amador Pérez-Tomás, Narcis Mestres, Moises Espindola-Rodriguez, Simon López-Marino, Markus Neuschitzer, "Multiwavelength excitation Raman scattering analysis of bulk and two-dimensional MoS_2 : vibrational properties of atomically thin MoS_2 layers", 2D Materials, 2, 035006, 2015.,

[19] K. Gołasa, M. Grzeszczyk, P. Leszczynski, C. Faugeras, A. A. L. Nicolet, A. Wysmołek, M. Potemski, and A. Babinski, "Multiphonon resonant Raman scattering in MoS_2", Applied Physics Letters, 104, 092106, 2014.

[20] Y. Zhang, T.T. Tang, C. Girit, Z. Hao, M. C. Martin, A. Zettl, M. F. Crommie, Y. R. Shen, and F. Wang, "Direct observation of a widely tunable bandgap in bilayer graphene", Nature 459, 820 (2009).

[21] Y. Cheng, Z. Zhu, and U. Schwingenschlogl, "Role of interlayer coupling in ultra-thin MoS_2", RSC Adv.,2, 7798, 2012.

[22] D. Gopalakrishnan, D. Damien, and M. M. Shaijumon, "MoS_2 Quantum Dot-Interspersed Exfoliated MoS_2 Nanosheets", ACS Nano, 8, 5297, 2014.

[23] J. P. Wilcoxon and G. A. Samara, "Strong quantum-size effects in a layered semiconductor: MoS_2 nanoclusters", Phys. Rev. B, 51, 7299, 1995.

[24] J. P. Wilcoxon, P. P. Newcomer, and G. A. Samara, "Synthesis and optical properties of MoS2 and isomorphous nanoclusters in the quantum confinement regime", Journal of Applied Physics, 81, 7934, 1997.

[25] V. Chikan and D. F. Kelley, "Size-Dependent Spectroscopy of MoS_2 Nanoclusters", J. Phys. Chem. B, 106, 3794, 2002.